CORRELATION OF SPACE DEBRIS OBSERVATIONS BY THE VIRTUAL DEBRIS ALGORITHM

G. Tommei[1], A. Milani[1], D. Farnocchia[1], and A. Rossi[2]

[1] *Department of Mathematics, University of Pisa, Largo Pontercorvo 5, Pisa, Italy*
[2] *ISTI-CNR, Via Moruzzi 1, Pisa, Italy*

ABSTRACT

The main problem in the orbit determination of the space debris population is the correlation of independently observed tracklets, that are sets of observations over a short time. The information contained in such data are not sufficient for a complete determination of an orbit, thus we need to find two or more tracklets belonging to the same physical object and an orbit fitting all the observations. In this paper we will show how to use the admissible region tool to generate a set of virtual objects (Virtual Debris) which can be used as alternate preliminary orbits and as starting points for a recursive procedure of correlation. We shall focus on optical observations of GEO showing some preliminary results testing the 2007 data by the ESA Optical Ground Station (OGS) at Teide Observatory (Canary Islands), after an astrometric reduction performed by University of Bern.

Key words: orbit determination; correlation; virtual debris.

1. INTRODUCTION

A *tracklet* is a set of observations over a short time, assembled because they are nearby and aligned, thus believed to belong to the same satellite/debris. The main problem is the correlation of independently observed tracklets, because one tracklet is generally not enough to determine an orbit. The same problem is called identification in the context of asteroid surveys, and has recently been solved as part of the preparatory work for the next generation astronomical surveys Pan-STARRS and LSST [4]. The same technique can be applied, with appropriate modifications, to the space debris correlation problem [5].

From a tracklet we fit an *attributable*, a 4-dimensional vector synthesizing the information from the observations (Section 2). Then we compute the *admissible region* for the undetermined quantities range and range-rate corresponding to orbits which could be possible for Earth orbiting objects (as opposed to both interplanetary orbits and ballistic ones) (Section 3). This region is sampled by an optimal Delaunay triangulation generating a swarm of *Virtual debris* (VD), that is a set of possible, but by no means determined, set of six quantities assigning an orbit (Section 4). Each virtual debris is then propagated to the epochs for which other tracklets are available, and they are all tested for attribution to the orbit. If this correlation satisfies a suitable statistical quality control, a differential correction procedure is started to fit all the observations from both tracklets (Section 5). Given a successful 2-tracklet orbit, it is used to test possible attributions of other tracklets, and so on recursively (Section 6).

The software developed for the space debris case has been validated using data obtained by the ESA Optical Ground Station (OGS) at Teide Observatory (Canary Islands) in the year 2007. In Section 7 we shall analyze the results of the application of our method.

2. TRACKLETS AND ATTRIBUTABLES

A tracklet is a set of astrometric observations belonging to the same object (they fit to some smooth curve, typically a low degree polynomial):

$$t_i, \alpha_i, \delta_i, h_i \qquad i = 1, m \qquad m \geq 2$$

where α_i, δ_i are angles (usually right ascension and declination) and t_i are times, with $t_i < t_{i+1}$; the quantities h_i are the values of the apparent magnitude. Data from one tracklet are not generally sufficient for the determination of an orbit with classical methods, but it is possible to synthesize the information contained in the tracklet by an attributable. An attributable is a vector

$$A = (\alpha, \delta, \dot{\alpha}, \dot{\delta}) \in [-\pi, \pi) \times (-\pi/2, \pi/2) \times \mathbb{R}^2 \,,$$

representing the angular position and velocity of the body at a time $\bar{t} = Mean\,(t_i)$ in the selected reference frame.

Given the observed values $(t_i, \alpha_i, \delta_i)$ for $i = 1, m$ with $m \geq 2$, we can compute an attributable with its uncertainty fitting both angular coordinates with linear functions of time. More precisely, let the fit solution at time $\bar{t}$ be $(\alpha, \dot{\alpha}, \delta, \dot{\delta})$: this solution is obtained with the

Proc. '5th European Conference on Space Debris', Darmstadt, Germany 30 March – 2 April 2009, (ESA SP-672, July 2009)

regression line formulas, together with the two 2×2 normal matrices $C_{(\alpha,\dot\alpha)}, C_{(\delta,\dot\delta)}$ and covariance matrices $\Gamma_{(\alpha,\dot\alpha)}, \Gamma_{(\delta,\dot\delta)}$. The normal matrix C_A of A is composed just by joining the two normal matrices, and is not singular provided the observations refer to ≥ 2 distinct times; its inverse Γ_A is also composed by joining the two 2×2 covariance matrices.

A set of observations giving an attributable is not enough to compute an orbit, unless some restrictive hypothesis is used. In fact with these data we have a 2-dimensional manifold of possible orbits that give exactly the same attributable at a given time. Thus to complete an orbit we need either to assume 2 coordinates, or to set 2 constraints, e.g., assuming a *circular orbit*, that is a good approximation for geostationary objects but not for geosynchronous ones, which may have a significant eccentricity. In the next sections we shall explain how to use the information contained in the attributable in order to compute orbits.

3. ADMISSIBLE REGION FOR EARTH SATELLITES

Starting from an attributable, we would like to extract sufficient information from it in order to compute preliminary orbits: we shall use the admissible region tool, as described in [5].

The admissible region replaces the conventional confidence region as defined in the classical orbit determination procedure. The main requirement is that the geocentric energy of the object is negative, that is the object is a satellite of the Earth.

Given the geocentric position $\mathbf{r}$ of the debris, the geocentric position $\mathbf{q}$ of the observer, and the topocentric position $\boldsymbol{\rho}$ of the debris we have $\mathbf{r} = \boldsymbol{\rho} + \mathbf{q}$ and the energy (per unit of mass) is given by

$$\mathcal{E}_\oplus(\rho, \dot\rho) = \frac{1}{2}\|\dot{\mathbf{r}}(\rho, \dot\rho)\|^2 - \frac{\mu_\oplus}{r(\rho)}\,, \tag{1}$$

where $\mu_\oplus$ is the Earth gravitational parameter. Then a definition of admissible region such that only satellites of the Earth are allowed includes the condition

$$\mathcal{E}_\oplus(\rho, \dot\rho) \leq 0 \tag{2}$$

that could be rewritten as

$$2\mathcal{E}_\oplus(\rho, \dot\rho) = \dot\rho^2 + c_1\dot\rho + T(\rho) - \frac{2\mu_\oplus}{\sqrt{S(\rho)}} \leq 0\,, \tag{3}$$

where

$$\begin{aligned} S(\rho) &= \rho^2 + c_5\,\rho + c_0\,, \\ T(\rho) &= c_2\,\rho^2 + c_3\,\rho + c_4 \end{aligned}$$

and coefficients c_i depending on the attributable. In order to obtain real solutions for $\dot\rho$ the discriminant of $2\,\mathcal{E}_\oplus$ (polynomial of degree 2 in $\dot\rho$) must be non-negative:

$$\Delta_\oplus = \frac{w_1^2}{4} - T(\rho) + \frac{2\,\mu_\oplus}{\sqrt{S(\rho)}} \geq 0\,.$$

This observation results in the following condition on ρ:

$$\frac{2\mu_\oplus}{\sqrt{S(\rho)}} \geq Q(\rho)\,, \tag{4}$$

where

$$Q(\rho) = w_2\,\rho^2 + w_3\,\rho + \gamma\,,$$

with

$$\gamma = w_4 - \frac{w_1^2}{4}\,.$$

Condition (4) can be seen as an inequality involving a polynomial $V(\rho)$ of degree 6:

$$V(\rho) := Q^2(\rho)S(\rho) \leq 4\,\mu_\oplus^2\,. \tag{5}$$

Studying the polynomial $V(\rho)$ and its roots, as done by [3], the conclusion is that the region $\mathcal{C}_1$, defined by condition (2), can admit more than one connected components, but it has at most two. The qualitative structure of the confidence region is shown in Figure 1.

The admissible region needs to be compact in order to have the possibility to sample it with a finite number of points, thus a condition defining an inner boundary needs to be added. The choice for the inner boundary depends upon the specific orbit determination task: a simple method is to add constraints $\rho_{min} \leq \rho \leq \rho_{max}$ allowing, e.g., to focus the search of identifications to one of the three classes LEO, MEO and GEO. Another natural choice for the inner boundary is to take $\rho \geq h_{atm}$ where h_{atm} is the thickness of a portion of the Earth atmosphere in which a satellite cannot remain in orbit for a significant time span. As an alternative, it is possible to constrain the semimajor axis of the satellite to be larger that $R_\oplus + h_{atm} = \bar R$, and this leads to an equation

$$\mathcal{E}_\oplus(\rho, \dot\rho) \geq -\frac{\mu_\oplus}{2\,\bar R} \tag{6}$$

which defines another degree six inequality with the same coefficients but for a different constant term.

Another possible way to find an inner boundary is to exclude trajectories impacting the Earth in less than one revolution, that is to use an inequality on the perigee q [1]

$$q = a(1-e) \geq \bar R\,. \tag{7}$$

By substituting into the 2-body formulae involving the angular momentum $\mathbf{c} = \mathbf{c}(\rho, \dot\rho)$ we obtain

$$\sqrt{1 + \frac{2\mathcal{E}_\oplus\|\mathbf{c}\|^2}{G^2\,m_\oplus^2}} \leq 1 + \frac{2\mathcal{E}_\oplus\bar R}{\mu_\oplus}\,. \tag{8}$$

Since the left hand side is $e \geq 0$, we need to impose the condition

$$1 + \frac{2\mathcal{E}_\oplus\bar R}{\mu_\oplus} \geq 0$$

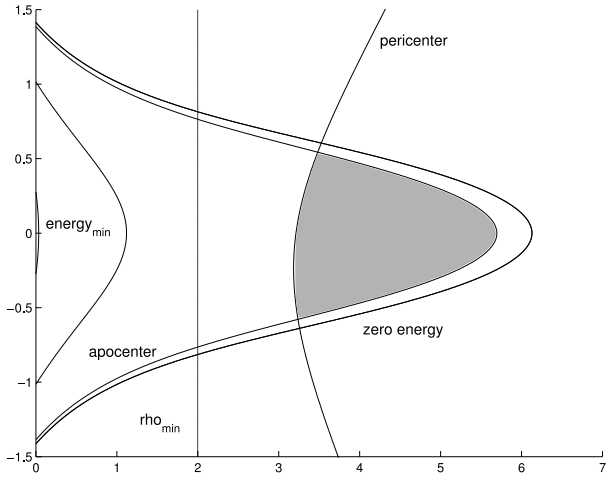

Figure 1. *Admissible region in the $(\rho, \dot{\rho})$ plane: the grey part contains the "good" orbits, that are geocentric orbits satisfying condition on pericenter and apocenter distance.*

on the right hand side: this is again $a \geq \bar{R}$. By squaring (8) we obtain

$$||\mathbf{c}||^2 \geq 2\,\bar{R}\,(\mu_\oplus + \mathcal{E}_\oplus \bar{R})\,. \tag{9}$$

The above condition is an algebraic inequality in the variables $(\rho, \dot{\rho})$; by another squaring it is possible to convert it into a polynomial equation of degree 10 in ρ and degree 4 in $\dot{\rho}$. Fig. 1 shows also this inner boundary, as well as an alternative outer boundary constraining the apocenter Q at some large value (the equations are analogous). The main limitation of this approach is that we do not have a rigorous proof that the number of components of a region defined by eqs. (7) and (2) has at most two connected components.

4. ATTRIBUTABLE ELEMENTS

The admissible region can be used to generate a swarm of virtual debris: we sample it starting from its boundary. We would like to select points that are equispaced on the boundary, that is, if the boundary is parameterized by its arc length s, then the distance of each couple of consecutive points corresponds to a fixed increment of s. To avoid the computation of the arc length parameter we use the following idea: we choose a large number of points, equispaced in one of the two coordinates, and then we use an elimination rule to be iterated until we are left with the desired number of points. It can be shown [3] that the remaining points are close to the ideal distribution, equispaced in arc length. Identified the polygonal domain $\tilde{\mathcal{D}}$ defined by connecting with edges the sample of boundary points of the admissible region $\mathcal{D}$ we triangulate it. Among all possible triangulations of $\tilde{\mathcal{D}}$ domain we chose the *constrained Delaunay triangulation* which has some optimum properties (see Fig. 2).

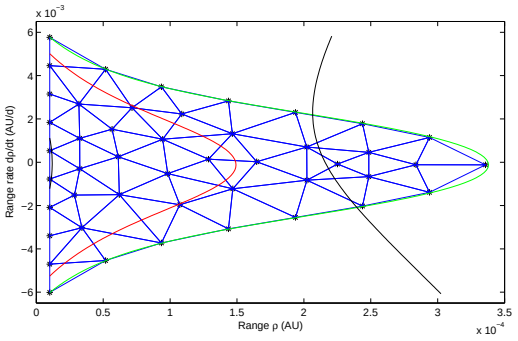

Figure 2. *Triangulated admissible region for an attributable computed by a tracklet of the OGS data. The green curve is the curve of zero energy, the blue points are the nodes of the triangulation, the red curve is the curve of minimal energy and the black curve is the curve of minimal pericenter.*

Each node of the triangulation defines a virtual debris, that is a possible, but by no means determined, set of six quantities

$$X^i = (\alpha, \delta, \dot{\alpha}, \dot{\delta}, \rho_i, \dot{\rho}_i) = (A, B^i)$$

composed by the attributable and the values of range and range rate. A set of six initial conditions uniquely determines the orbit of a debris, thus it is a set of orbital elements, belonging to a new type (different from the classical coordinates, such as Keplerian, equinoctial, cometary, Cartesian, etc.). We shall call such data a set of *attributable orbital elements*.

5. CORRELATION ALGORITHM

We assume that for a given debris object the only observational information available is contained in two attributables, A_1 at time $\bar{t}_1$ and A_2 at time $\bar{t}_2$. Neither from the first nor from the second we can compute an orbit, thus we have a *correlation* problem.

The idea is to generate a swarm of virtual debris X^i, sampling as described in the previous section the confidence region of one of the two attributables, let us say A_1. Then we compute, from each of the X^i, a prediction A^i for the epoch $\bar{t}_2$, each with its covariance matrix Γ_{A^i}. Generically these covariance matrices will be invertible, and the corresponding normal matrices C_{A^i} can be computed. We also know the normal matrix C_2 of the attributable A_2. Thus for each virtual debris X^i we can compute an *attribution penalty* K_4^i (see [2]) and use the values as a criterion to select some of the virtual asteroids to proceed to the orbit computation. Note that the identification penalty K_4^i, computed for a given node B_1^i of the triangulation of A_1, does not need to be small. First, we cannot know a priori whether the two objects observed at times $\bar{t}_1$ and $\bar{t}_2$ are indeed the same. Second, even if they were the same, the value of B_1^i could be totally wrong with respect to the true values of the distance and its derivative

at time $\bar{t}_1$. In both cases the two attributables cannot fit, and this will be revealed by a large value of K_4^i.

Thus the procedure might be as follows. If for all nodes i the value of the penalty is large, say K_4^i greater than some maximum K_{max}, then we discard the couple (A_1, A_2) as not likely to belong to the same body. If there are some nodes B_1^i such that $K_4^i \leq K_{max}$, then we proceed to the next step.

The value of the control K_{max} to be used is difficult to establish a priori, because we lack an analytical theory. We cannot use χ^2–tables for dimension 8, because we are sampling the confidence region with a finite number of points B_1^i, thus we cannot assume that the minimum among the K_4^i is the absolute minimum we could get by trying all values of $B_1 \in \mathcal{D}(A_1)$, that is

$$Min_{i=1,k} K_4^i \geq Min_{B_1 \in \mathcal{D}(A_1)} K_4(A_1, B_1) \qquad (10)$$

and we cannot compute analytically the safety margin to be left to take into account this difference. We conclude that the value of K_{max} to be used in large scale production of correlations can only be dictated by the analysis of the results of large scale tests.

The procedure described above provides us also with a number of best fitting corrected attributables A_2^i.

Each A_2^i comes with its penalty value K_4^i, which is not too large, that is, an orbit with B_1^i as distance and radial velocity at time t_1^i and giving the attributable A_2^i as observation at time $\bar{t}_2$, can fit both A_1 and A_2 with not too large residuals; the fit is performed in the 8-dimensional space of the residuals of both attributables.

To start differential corrections we need a preliminary orbit that is a set of orbital elements to be used as first guess. There is no requirement that such an orbit is accurate: it is only hoped that it belongs to the convergence domain of the differential corrections. To achieve this, we have a number of options, the simpler one is to use attibutable orbit elements (Section 4) composed by the attributable A_2^i and the value $B_2^i = (\rho_2^i, \dot{\rho}_2^i)$ as computed from the orbit $X^i = [A_1, B_1^i]$ at t_1^i. The epoch of this set of initial conditions is $\bar{t}_2 - \rho_2^i/c$.

We have validated this algorithm by running it on the 3172 tracklets provided to us from the 2007 OGS observations: we correlated 267 tracklets obtaining 109 orbits (see Sec.6).

Since the astrometric prediction function is nonlinear, and there is no guarantee that if the time $\bar{t}_2$ is very far from $\bar{t}_1$, this algorithm works properly we have limited the time interval to less than one day, that is less than one orbital period.

The accepted preliminary orbits are used as starting guess for differential corrections; if they are convergent, we accept the 2-tracklet correlation with the orbit from the least squares fit.

6. CORRELATION CONFIRMATION

Correlation confirmation is best obtained by looking for a third tracklet which can also be correlated to the other 2; this process is called *attribution*. From the available 2-tracklets orbit with covariance we predict the attributable A_P at the time $\bar{t}_3$ of the third tracklet, and compare with the attributable A_3 computed from the third tracklet. Since both A_p and A_3 come with a covariance matrix, we can compute the χ^2 of the difference and use it as a test, then proceed to differential corrections [4].

The procedure is *recursive*, that is we can use the 3-tracklet orbit to search for attribution of a fourth tracklet, and so on. This generates a very large number of many-tracklets orbits, but there are many duplications, corresponding to adding the tracklets in a different order.

By correlation management we mean a procedure to remove duplicates (e.g., $A = B = C$ and $A = C = B$) and inferior correlations (e.g., $A = B = C$ is superior to both $A = B$ and to $C = D$, thus both are removed). The output catalog after this process is called normalized.

The output of our test with the 2007 OGS data, after correlation management, included 109 correlations.

T	2	3	4	Total
C	69	31	9	109

Table 1. C is the number of correlations found with T tracklets

The 2007 observations were not scheduled to allow for orbit determination and in particular there are few objects having at least two tracklets in a single night; thus a lot of tracklets remain uncorrelated.

Of course we have no way to know how many should have been correlated, that is how many physically distinct objects are there: in particular, objects re-observed at intervals longer than 10 days have escaped correlation.

7. DATA ANALYSIS

In this section we shall examine the results obtained applying our algorithm to real data. The data we have used have been obtained by the ESA Optical Ground Station (OGS) at Teide Observatory (Canary Islands) in the year 2007. They were collected in a survey targeted at the geosynchronous belt, although of corse objects in different orbits were incidentally imaged; the region being suveyed was a belt above and below the *geosynchronous line*, where exactly circular, equatorial and geosynchronous orbits could be seen from the OGS location. Fig. 3 shows a global view of this data set in a body-fixed reference frame.

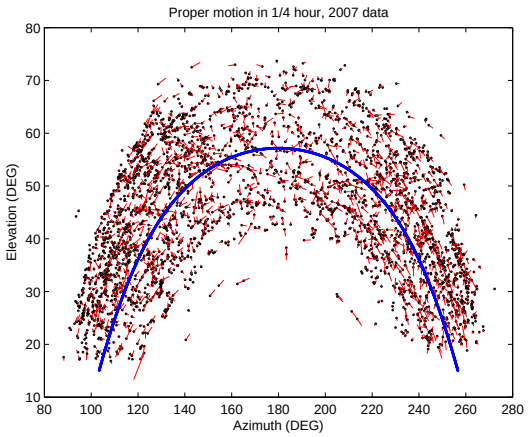

Figure 3. *Validation dataset: 2007 tracklets from ESA OGS, preprocessed by University of Bern. Angles are in a body-fixed altazimutal reference. Angular velocity is represented by the motion in 1/4 hour. The blue line is the geostationary line (where GEO with $e = I = 0$ are found).*

The population which is observed by surveying around the geostationary line contains geostationary objects, with low values of e and I and geosynchronous (or almost) objects which could have a significant e and I, including some very high values which could occur for large Area/Mass (A/M) as a result of radiation pressure [6].

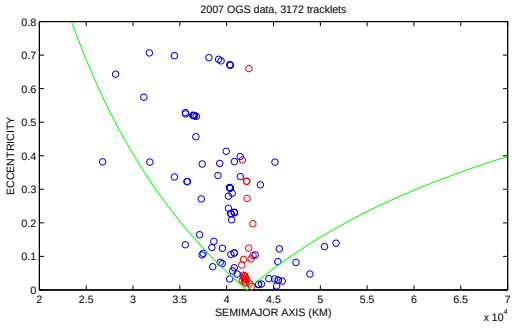

Figure 4. *Orbits determined with our method projected on the (a, e) plane: the green lines indicate apocenter (on the left) and pericenter (on the right) at the geostationary altitude.*

Some of the observed tracklets give origin to orbits with semimajor axis very different from the GEO, orbits probably belonging to drifting objects.

The orbits in the (a, e) (Fig. 4) plane show a concentration of GEO orbits, including some with high eccentricity.

Fig. 5 shows that there are two groups of orbits with $e \simeq 0.32$ and $e \simeq 0.41$, and they also correspond to a quite large inclination: $I \simeq 17°.5$ and $I \simeq 10°$. These value could be reached in few years by originally geostationary debris provided they have A/M of the order of

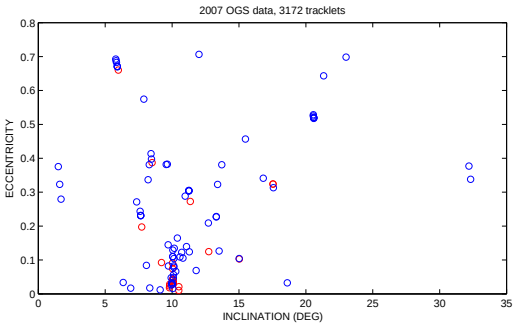

Figure 5. *Orbits from our method projected on the (I, e) plane: the red dots are nearly geosynchronous orbits, with a within 700 km from the geosynchronous value. The few GEO orbits with high e and I should have high area/mass ratio.*

20 m^2/kg [6]. The two groups of orbits actually correspond to just two objects, because the correlation was not achieved. For the values of A/M cited above, the radiation pressure perturbation is much larger than the ones due to Earth's spherical harmonics, the Moon and the Sun. Thus a least squares fit over a time span of many days must necessarily fail, unless we have a radiation pressure model. For now we have only order of magnitude guesses for the radiation pressure model parameters, including A/M (but not only, since the shapes are certainly not spherical). If we had a much larger data set of observations of these objects, we could estimate the values of these parameters and presumably correlate all the observations of these two objects.

Fig. 5 shows an apparent lack of really geostationary orbits, with low e and I: actually there is only one orbit with $e < 0.01$ and $I < 2°$. This is due to the fact that the survey conducted by the OGS in 2007 had the purpose of discovering new objects, and the geostationary objects are mostly active satellites, whose orbits and ephemerides are known. Thus the fields of view were on purpose avoiding the geostationary line of Fig. 3.

Fig. 6 and 7 show the distribution of eccentricity/inclination versus intrinsic luminosity of the objects, the latter described in the absolute magnitude scale. Unfortunately it is not easy to convert an absolute magnitude into a size, because of the wide range of albedo values and also because of irregular shapes. However, if we could assume albedo 0.1 and a spherical shape, we would get a diameter ranging between 10 m and $\simeq 30$ cm for the correlated objects. Thus the largest objects should be full satellites (at low e) and rocket stages, the smallest are certainly debris.

The existence of objects with high e and also I was already well known, what is interesting is that some of these have a quite large cross section. To understand the dynamics of such objects is a challenge, which requires advanced models and a good data set of both astrometry and photometry.

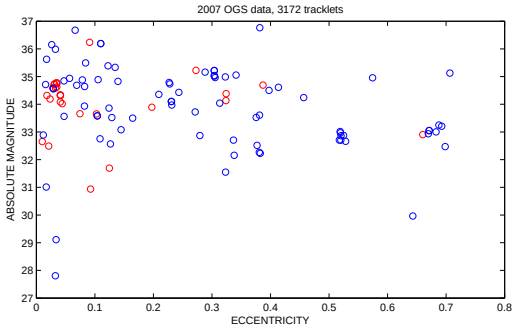

Figure 6. Orbits from our method projected on the (e, H) plane, where H is the absolute magnitude. $H = 28$ would correspond to about 10 m diameter, $H = 33$ to 1 m, if the shape was spherical and albedo was 0.1, like the one of the average asteroid. The largest objects should be satellites (lower left) and rocket stages (lower right).

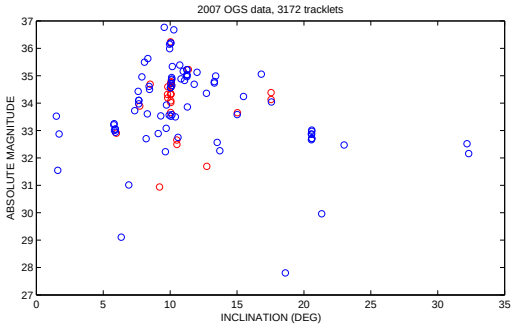

Figure 7. Orbits determined with our method projected on the (I, H) plane. There is a geosynchronous population with moderately high inclination, and a wide range of sizes.

8. CONCLUSIONS AND FUTURE WORK

1. We have developed and validated with one year of OGS data an orbit determination method, already theoretically described in [5]; this method requires two tracklets per night and computes full orbits, with 6 elements. For a method requiring 1 tracklet per night, see the paper by Milani et al. in these proceedings.

2. We find a certain number of correlations, even in a dataset which was taken without following a strategy optimized for orbit determination and in particular for this method (few objects with at least two tracklets per night). The resulting orbits make sense, thus most of them should be right, although a few may be wrong (especially the ones not confirmed by correlating a third tracklet).

3. The resulting catalog of orbits is not yet in a 1-1 correspondence with real objects, because objects observed too far apart in time cannot be fit to a purely gravitational orbit. This phenomenon is especially relevant for large area/mass objects (with $A/M \simeq 1$ m^2/kg, the radiation pressure is as important as the J_2 perturbation, see [6], Fig. 1).

4. This method also applies with radar data, provided the radar measures $(\rho, \dot{\rho}, \alpha, \delta)$ gives us a 4-dimensional radar attributable [2, 1]. In this case the admissible region has a simple shape, a conic [5].

ACKNOWLEDGMENTS

These results are from the ESOC Contract No. 21280/07/D/CS, "Orbit Determination of Space Objects Based on Sparse Optical Data", including the validation tests, for the algorithms described above, based on one year of data from the ESA OGS telescope. We thank the University of Bern (in particular T. Schildknecht) and ESA for providing these data and for supporting our research.

REFERENCES

[1] Farnocchia, D. (2008). Orbite preliminari di asteroidi e satelliti artificiali. Master Thesis, University of Pisa.

[2] Milani, A. & Gronchi G. F. (2009). *The theory of orbit determination*, Cambridge University Press.

[3] Milani, A., Gronchi, G. F., De' Michieli Vitturi, M. and Knezevic, Z. (2004). Orbit Determination with Very Short Arcs. I Admissible Regions. *Celestial Mechanics & Dynamical Astronomy*, **90**, pp. 57-85

[4] Milani, A., Gronchi, G. F., Knezevic, Z., Sansaturio M. E. and O. Arratia (2005). Orbit determination with very short arcs. II Identifications. *Icarus*, **179**, pp. 350-374

[5] Tommei, G., Milani, A. and Rossi, A. (2007). Orbit Determination of Space Debris: Admissible Regions. *Celestial Mechanics & Dynamical Astronomy*, **97**, pp. 289 - 304

[6] Valk, S., Lemaitre, A., Anselmo, L. (2007) Analytical and semi-analytical investigations of geosynchronous space debris with high area-to-mass ratios influenced by solar radiation pressure. *Adv. Space Res.* **41**, 1077–1090.